Histamine H_1 receptor activation blocks two classes of potassium current, $I_{K(rest)}$ and I_{AHP}, to excite ferret vagal afferents

M. Samir Jafri, Kimberly A. Moore, Glen E. Taylor and Daniel Weinreich*

University of Maryland, School of Medicine, Department of Pharmacology and Experimental Therapeutics, 685 West Baltimore Street, Baltimore, MD 21201-1559, USA

1. Intracellular recordings were made in intact and acutely dissociated vagal afferent neurones (nodose ganglion cells) of the ferret to investigate the membrane effects of histamine.

2. In current-clamp or voltage-clamp recordings, histamine (10 μM) depolarized the membrane potential (10 $\pm$ 0·8 mV; mean $\pm$ S.E.M.; $n = 27$) or produced an inward current of 1·6 $\pm$ 0·35 nA ($n = 27$) in ~80% of the neurones.

3. Histamine (10 μM) also blocked the post-spike slow after-hyperpolarization (AHP_{slow}) present in 80% of these neurones (95 $\pm$ 3·2%; $n = 5$). All neurones possessing AHP_{slow} in ferret nodose were C fibre neurones; all AHP_{slow} neurones had conduction velocities $\leqslant 1$ m s^{-1} ($n = 7$).

4. Both the histamine-induced inward current and the block of AHP_{slow} were concentration dependent and each had an estimated EC_{50} value of 2 μM. These histamine-induced effects were mimicked by the histamine H_1 receptor agonist 2-(2-aminoethyl)thiazole dihydrochloride (10 μM) and blocked by the H_1 antagonists pyrilamine (100 nM) or diphenhydramine (100 nM). Schild plot analysis of the effect of pyrilamine on the histamine-induced inward current revealed a pA_2 value of 9·7, consistent with that expected for an H_1 receptor. Neither impromidine (10 μM) nor $R(-)$-α-methylhistamine (10 μM), selective H_2 or H_3 agonists, respectively, significantly affected the membrane potential, input resistance or AHP_{slow}.

5. The reversal potential (V_{rev}) for the histamine-induced inward current was $-84 \pm 2·1$ mV ($n = 4$). The V_{rev} for the histamine response shifted in a Nernstian manner with changes in the extracellular potassium concentration. Alterations in the extracellular chloride concentration had no significant effect on the V_{rev} of the histamine response ($n = 3$). The V_{rev} for the AHP_{slow} was $-85 \pm 1·7$ mV ($n = 4$).

6. These results indicate that histamine increases the excitability of ferret vagal afferent somata by interfering with two classes of potassium current: the resting or 'leak' potassium current ($I_{K(rest)}$) and the potassium current underlying a post-spike slow after-hyperpolarization (I_{AHP}). Both these effects can occur in the same neurone and involve activation of the same histamine receptor subtype, the histamine H_1 receptor.

Vagal primary afferent neurones carry mechanical, thermal and chemical sensory information from the viscera to the central nervous system. In the periphery this transfer of information can be modulated by a wide variety of inflammatory mediators (Baccaglini & Hogan, 1983; Leal-Cardoso, Koschorke, Taylor & Weinreich, 1993; Undem & Weinreich, 1993; also reviewed by Marshall & Waserman, 1995; Undem & Riccio, 1997). Histamine is a prototypic inflammatory mediator released from mast cells near peripheral sensory terminals of vagal afferent neurones (Wasserman, 1994). Once released, histamine can provoke a wide range of inflammatory effects including stimulation of vagal C fibre neurones *in vivo* (Coleridge & Coleridge, 1977). Histamine is also contained in and released from mast cells present in vagal sensory ganglia (Undem, Hubbard & Weinreich, 1993). These ganglia, the inferior and superior vagal ganglia (nodose and jugular ganglia, respectively) contain somata that give rise to vagal afferent axons.

* To whom correspondence should be addressed.

In the guinea-pig, immunological activation of mast cells in nodose ganglia *in vitro* results in the release of sufficient quantities of histamine to depolarize the resting membrane potential and change the resting membrane conductance in the majority of neurones (Undem *et al.* 1993). Histamine can depolarize the resting membrane potential and change the resting membrane conductance of vagal afferents in many species including rabbit (Higashi, Ueda, Nishi, Gallagher & Shinnick-Gallagher, 1982; Leal-Cardoso *et al.* 1993) and guinea-pig (Undem & Weinreich, 1993). These observations indirectly imply a role for histamine in sensitizing chemosensitive reflexes mediated by vagal afferents.

Despite the fact that histamine can excite most vagal afferent neurones, the nature of the membrane ionic channels mediating the excitatory effects of this inflammatory mediator is largely unknown. In nodose neurones from the ferret, we observed that histamine produced a robust membrane depolarization and an associated decrease in membrane conductance. In the current work we have examined in depth this effect of histamine. We show that histamine depolarizes the membrane by blocking a potassium current that is active at rest ($I_{K(rest)}$). In addition we report that histamine decreases the accommodative properties of these neurones through a block of the post-spike slow after-hyperpolarization (AHP_{slow}). Both these actions of histamine are mediated through activation of the same histamine receptor subtype, the histamine H_1 receptor.

METHODS

Preparation of tissue

Nodose ganglia were isolated from adult male ferrets (1–2 kg) purchased from Marshall Farms USA Inc. (North Rose, NY, USA). After the animals were killed by CO_2 asphyxiation followed by exsanguination, the ganglia were removed and placed in 4 °C Locke solution of the following composition (mM): 136 NaCl, 5·6 KCl, 14·3 $NaHCO_3$, 1·2 NaH_2PO_4, 2·2 $CaCl_2$, 1·2 $MgCl_2$ and 10 dextrose; equilibrated continuously with 95% O_2–5% CO_2; pH 7·2–7·4. Ganglia were enzymatically dissociated on the day of dissection using the procedure described by Christian, Togo, Naper, Koschorke, Taylor & Weinreich (1993). Briefly, the ganglion was desheathed, cut into three to four pieces and placed in Ca^{2+}-free, Mg^{2+}-free Hanks' balanced salt solution (CMFH) of the following composition (mM): 138 NaCl, 5·0 KCl, 4·0 $NaHCO_3$, 0·3 Na_2HPO_4, 0·3 KH_2PO_4, 5 dextrose and 0·03 Phenol Red. All incubations were done at 37 °C. The pieces of tissue were incubated for 7 min in 10 ml CMFH containing papain (100 μl, 0·1 mg ml^{-1}; Boehringer Mannheim) which was activated by L-cysteine (0·2 mg ml^{-1}; Sigma). The tissue was then washed twice with CMFH and incubated for 10 min in 4 ml CMFH containing dispase (grade II, 2 mg ml^{-1}; Boehringer Mannheim) and collagenase (Type 1A, 1 mg ml^{-1}; Sigma). During the incubation the tissue was triturated with a fire-polished Pasteur pipette at 8 and 10 min. After washing twice with Leibovitz L-15 medium (Gibco) containing 10% (v/v) fetal bovine serum (FBS; JRH Biosciences, Lexena, KS, USA), cells were resuspended in 150 μl L-15–10% FBS per coverslip. A 24-well culture plate was prepared by placing a 15 mm poly-D-lysine-coated coverslip in the bottom of each well. After resuspension, 150 μl of the cell suspension was added to each well. Neurones were allowed to settle and attach overnight at 37 °C before use. Recordings were performed on neurones within 48 h of plating. The Institutional Animal Care and Use Committee has approved all methodology used in these experiments.

Electrophysiological studies

Intracellular microelectrodes were fabricated from aluminosilicate capillary glass (1·0 mm o.d., 0·68 mm i.d.; Sutter Instruments, San Francisco, CA, USA) on a Brown–Flaming puller (Sutter) and backfilled with a solution of 3 M KCl (20–40 MΩ). The microelectrode was connected to an Axoclamp-2A amplifier (Axon Instruments). The discontinuous current injection mode (switching frequency, 5–6 kHz) of the amplifier was used for both current-clamp and voltage-clamp applications; the headstage voltage was monitored continuously to ensure that the sampled voltage reached steady state. Current and voltage outputs were viewed on-line on an oscilloscope and chart recorder and digitized with a Neurocorder (Neurodata Instruments, New York) for storage on videocassette tapes for off-line analysis. Data acquisition and voltage-clamp protocols were controlled using pCLAMP 5 or pCLAMP 6 software (Axon Instruments).

To measure the AHP_{slow}-associated current (I_{AHP}), a hybrid voltage-clamp technique was employed (Fig. 5*A*, bottom panel). Four depolarizing current spikes (2 nA, 3 ms, 100 ms interspike interval) were delivered to a neurone, current clamped at its resting membrane potential, to elicit four action potentials. The amplifier was then switched electronically to voltage-clamp mode 100 ms after the last action potential to record the I_{AHP} at a pre-set holding potential.

Neurones were superfused with oxygenated Locke solution (3–4 ml min^{-1}) at room temperature (20–22 °C). The superfusate level was lowered to approximately 50 μm above the surface of the neurones to minimize electrode stray capacitance. A neurone was judged acceptable for study if its resting membrane potential (< −50 mV) and action potential overshoot (above 0 mV) remained stable for 5 min after impalement. In experiments where input resistance or membrane conductance was assessed, square-wave current (−0·1 to −1·0 nA) or voltage (−5 or −10 mV) transients (250 ms duration), respectively, were applied throughout the experiment at 2·5 s intervals.

For intracellular measurement in nodose neurons from intact ganglia, ferret ganglia were prepared as previously described for rabbit and guinea-pig nodose neurones (Leal-Cardoso *et al.* 1993; Undem & Weinreich, 1993). For measurement of conduction velocities, intact nodose ganglia with a length of the peripheral process (~4 cm) attached were prepared for intracellular recording. The peripheral process was stimulated via a suction electrode attached ~4 cm from the ganglion. The latency from stimulus to intracellular recording of an action potential from a ganglionic soma was measured and used to calculate the conduction velocity.

Preparation and delivery of solutions

In all experiments assessing the reversal potential of the histamine-induced depolarization, the extracellular solution contained 2 mM CsCl to block the hyperpolarization-activated h-current. For experiments using low extracellular chloride, NaCl (136 mM) was replaced with NaCl (45 mM) and sodium isethionate (91 mM; Sigma), adjusted to pH 7·4. To eliminate a shift in the junction potential (< 2 mV) during experiments in low chloride solutions, the bath was grounded through a 3 M KCl–agar bridge.

All solutions were prepared daily for experiments from stock aliquots which were stored at −20 °C. Reservoirs containing solutions of various drugs or Locke solution with modified ionic content were connected to the inflow line of the recording chamber by three-way valves which could rapidly divert the source of superfusion from the main reservoir. This means of drug delivery introduced a 15 s delay from the activation of the valve to arrival of the drug solution in the chamber.

Histamine dihydrochloride, pyrilamine maleate and diphenhydramine hydrochloride (DPH) were obtained from Sigma. *R*(−)-α-methylhistamine dihydrochloride (R-α-MeHA) was obtained from Research Biochemicals International (Natick, MA, USA). 2-(2-Aminoethyl)thiazole dihydrochloride (2-TH) was obtained from SmithKline Beecham (Philadelphia, PA, USA).

Data analysis

Data are expressed as means ± S.E.M. Statistical significance was assessed using Student's two-tailed, unpaired *t* test at the $P < 0.05$ level of significance. Figure construction and fitting of mathematical functions to data were accomplished with SigmaPlot software (Jandel Scientific, San Rafael, CA, USA).

A semilogarithmic plot of the concentration–response relationship was iteratively fit using the four-parameter logistic equation:

$$Y = \frac{(\max - \min)}{(1 + (x/EC_{50}))^{b}} - \min,$$

where Y is the response to x concentration of histamine, max and min are the maximum and minimum responses, EC_{50} is the histamine concentration at half-maximum response and b is the Hill coefficient using the Levenberg–Marquardt non-linear least-squares algorithm (SigmaPlot). The correlation coefficient, r, is indicated for all fits.

RESULTS

Effect of histamine on membrane potential and membrane conductance

The effect of histamine was examined on thirty-four acutely dissociated neurones of which ~80% responded with a membrane depolarization (27 of 34 neurones). Bath application of 10 μM histamine for 30 or 45 s produced a reversible membrane depolarization in twenty-seven neurones (Fig. 1*A*); the remaining neurones were unresponsive. The mean response was 10 ± 0·8 mV (range, 5–20 mV). In a separate set of experiments where thirty-five neurones were voltage clamped to −60 mV, 10 μM histamine produced an inward current of 1·6 ± 0·35 nA (range, 0·1–6·6 nA; Fig. 1*B*) accompanied by a decrease in membrane conductance (−35 ± 3·9%; range, −4 to −79%) in 27 of 35 neurones (~80%). In ~10% of the neurones, the histamine-induced inward current was accompanied by either an increase or no net change in membrane conductance; these neurones were excluded from this study.

An analogous histamine-induced depolarization of the membrane potential was confirmed in neurones in intact ferret nodose ganglia. Bath application of 10 μM histamine produced a mean depolarization of 10 ± 1·2 mV (range, 5–15 mV) in seven of twelve neurones from seven ganglia; the remaining neurones were unresponsive.

Histamine increases membrane excitability

A membrane depolarization accompanied by a decrease in membrane conductance can potentially increase the excitability of these neurones by bringing the membrane

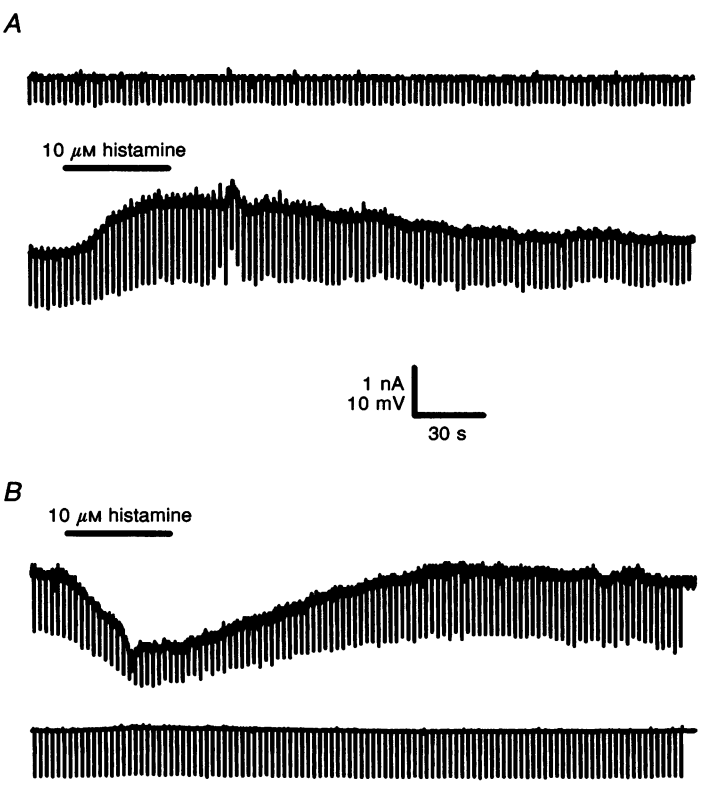

Figure 1. Effect of histamine on membrane properties in an acutely isolated adult ferret nodose neurone

Current (upper traces) and voltage (lower traces) records from current- or voltage-clamped histamine responses recorded in the same neurone. Negative deflections in these and all subsequent traces are produced by hyperpolarizing transmembrane current or voltage steps (−0·5 nA or −10 mV, 250 ms duration, 2·5 s interstep interval) to estimate membrane resistance or membrane conductance, respectively. *A*, a reversible membrane depolarization and associated increase in input resistance is elicited by superfusion of 10 μM histamine for 45 s (horizontal bar). Resting membrane potential was −70 mV. *B*, voltage-clamp recording in the same neurone showing an inward current and associated conductance decrease elicited by superfusion of 10 μM histamine for 45 s (horizontal bar). Holding potential was −60 mV.

potential closer to spike threshold and increasing the responsiveness of the neurone to depolarizing stimuli. To test this hypothesis, we applied a series of subthreshold to suprathreshold depolarizing current steps to current-clamped neurones in the absence (Fig. 2*A*) and presence of histamine (Fig. 2*B*). The number of incremental depolarizing current steps necessary to reach action potential threshold was greater in control than in the presence of 10 μM histamine. Under control conditions the minimum stimulus required to elicit an action potential was 643 $\pm$ 91·6 pA ($n = 7$) compared with a threshold value of 300 $\pm$ 90·0 pA ($n = 7$) in the presence of 10 μM histamine (Fig. 2*D*). The change in excitability can also be seen in a plot of the stimulus strength *versus* the latency of action potential generation under each condition (Fig. 2*C*). The leftward shift of the curve in the presence of 10 μM histamine indicates that smaller stimuli were sufficient to elicit action potentials more rapidly than in the absence of histamine. The excitability returns to control level following 5 min superfusion with histamine-free Locke solution (Fig. 2*C* and *D*). Both these assessments reflect the increased sensitivity of these neurones, such that previously subthreshold stimuli become suprathreshold in the presence of histamine.

Histamine-induced inward current results from blockade of $I_{K(rest)}$

To determine the ionic mechanisms involved in the histamine-induced depolarization, reversal potential (V_{rev}) values for the histamine-induced currents were estimated under various ionic conditions. The amplitude of the steady-state holding current was measured at varying pre-set membrane potentials in the absence and at the peak effect of 10 μM histamine application in the same neurone. The slope of this current–voltage (I–V) relationship in the presence of histamine is decreased reflecting a diminution

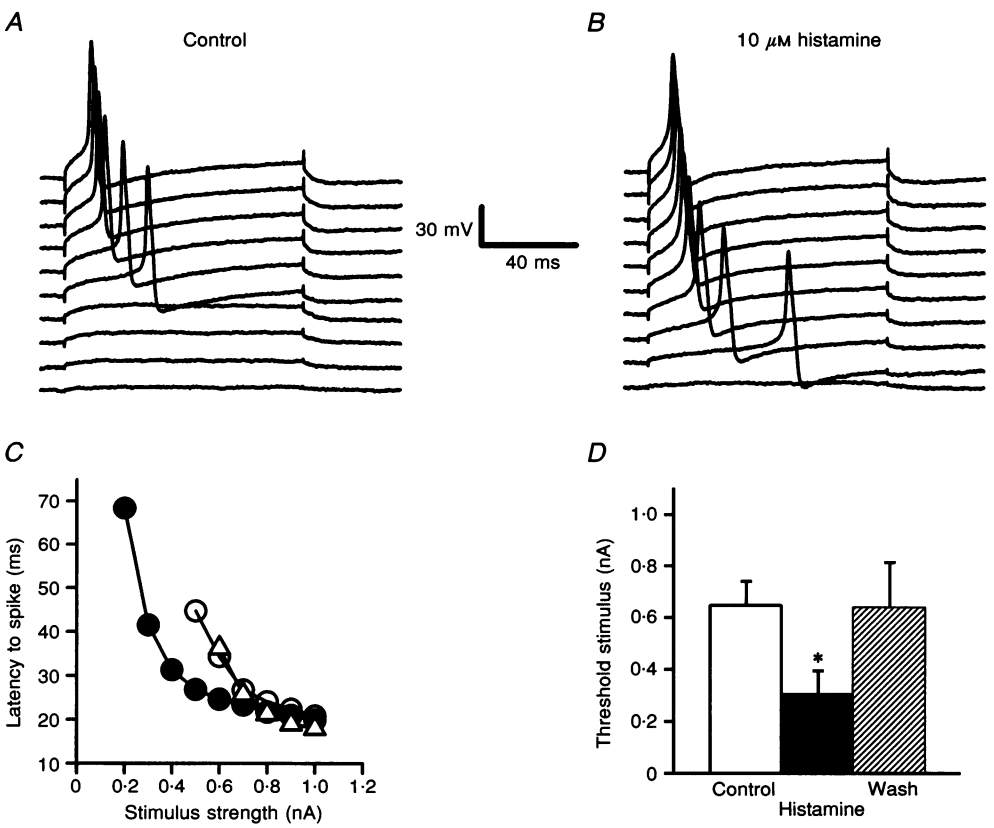

Figure 2. Strength–latency plot showing the increased excitability of a nodose neurone in the presence of histamine

Incremental 0·1 nA depolarizing current steps (0·1 to 1 nA, 100 ms duration, 5 s interstep interval) were applied to an isolated ferret nodose neurone current clamped to −63 mV in control Locke solution (*A*) and in Locke solution containing 10 μM histamine (*B*). The responses to current steps in the presence of histamine were recorded ~1 min after the start of histamine application, when the histamine response had reached steady state. Traces were offset for clarity; each step in the absence and presence of histamine was initiated from the same membrane potential. *C*, plot of stimulus strength *versus* latency to action potential in control Locke solution (○), in the presence of 10 μM histamine (●) or after 5 min wash out with histamine-free Locke solution (△). *D*, average threshold stimulus necessary to elicit an action potential in control Locke solution (□), in the presence of 10 μM histamine (■) or 5 min after washout of histamine (▨). Histamine significantly (* $P < 0·05$) decreased the stimulus strength necessary to elicit an action potential ($n = 7$).

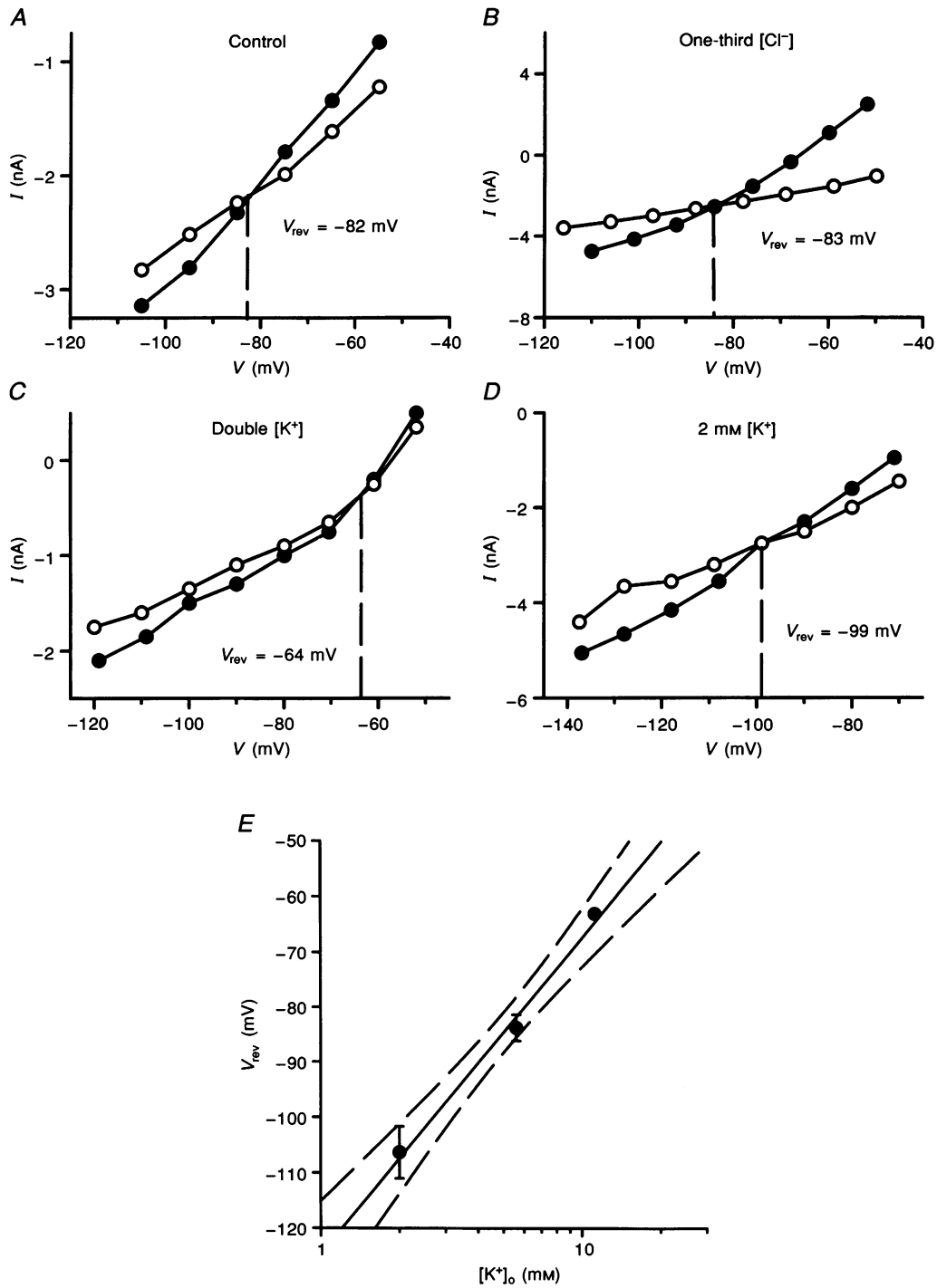

Figure 3. Effects of altering extracellular potassium concentration on the V_{rev} of the histamine-mediated current

A, *B*, *C* and *D* represent steady-state *I–V* relationships in the absence (●) or presence (○) of 10 μM histamine in Locke solution containing 5·6 mM (*A*), 11·2 mM (*C*) and 2 mM (*D*) potassium. *B*, represents a similar experiment with one-third normal chloride concentration. Neurones, voltage clamped to a holding potential of −60 mV, were subjected to a series of voltage step commands (250 ms), and the steady-state currents were recorded. Indicated V_{rev} values were measured as the potential at which the traces intersect (i.e. where the difference current is zero). Records *A–D* were recorded in different neurones. *E*, semi-logarithmic plot of the relationship between the $[K^+]_o$ and the mean (± S.E.M.) V_{rev} values for histamine-induced currents recorded in 3–4 neurones. The shift in the reversal potential value was linear ($r = 0{\cdot}962$) with a slope of 57 mV per decade change in $[K^+]_o$. The continuous line depicts the predicted Nernstian relationship between $[K^+]_o$ and V_{rev}. Dashed lines are the 95% confidence limits.

in membrane conductance produced by histamine. In the neurone illustrated in Fig. 3*A* the control and histamine *I–V* curves intersected at −82 mV. The mean V_{rev} value for the histamine response in four neurones was −84 ± 2·4 mV (range, −80 to −90 mV).

A depolarizing response accompanied by a decrease in membrane conductance with a V_{rev} value near −85 mV suggests that a decrease of a resting potassium conductance may underlie this response. To test this supposition the V_{rev} value of the histamine-induced current was measured in Locke solutions containing varying potassium concentrations. Superfusing neurones with Locke solution containing double the normal potassium (11·2 mM) yielded a V_{rev} value for the histamine-induced current of −63 ± 0·6 mV ($n = 3$; range, −62 to −64 mV; Fig. 3*C*). This 18 mV shift in the V_{rev} value was close to the 17 mV shift predicted by the Nernst equation. In Locke solution containing ~one-third normal potassium (2 mM), the V_{rev} values averaged −106 ± 2·7 mV ($n = 3$; range, −99 to −115 mV; Fig. 3*D*), near the predicted V_{rev} value of −111 mV. As depicted in Fig. 3*E*, the relationship between the extracellular potassium concentration and V_{rev} was linear ($r = 0{\cdot}962$) with a slope of −57 mV per decade that closely approximates the slope predicted by the Nernst equation. Reduction of extracellular chloride concentration to one-third normal had no effect on the reversal potential of the histamine response (−85 ± 1·8 mV; $n = 3$; range, −82 to −88 mV; Fig. 3*B*). These results support the hypothesis that the histamine-induced inward currents are largely, if not entirely, a result of a decrease in a resting potassium current.

Effect of histamine on AHP_{slow}

Previously, we have characterized AHP_{slow} in rabbit (Fowler, Greene & Weinreich, 1985) and guinea-pig nodose neurones (Undem & Weinreich, 1993). This long-duration (seconds), outward calcium-dependent potassium current hyperpolarizes the membrane potential and thus controls spike frequency adaptation (Weinreich, 1986; Weinreich & Wonderlin, 1987) in these neurones. An analogous AHP_{slow} is also present in > 80% of ferret nodose neurones (Figs 4*Aa* and 5*A*, top panel). All neurones possessing AHP_{slow} in the ferret, like those in the rabbit and guinea-pig, are C fibre neurones. When seven AHP_{slow} neurones in intact ganglia were tested for their conduction velocities, all had velocities $\leqslant 1\ m\ s^{-1}$.

Application of 10 μM histamine reversibly blocked the AHP_{slow} (95 ± 3·2%; $n = 5$; range, 82–100%; Fig. 8*B*). Block of the AHP_{slow} in rabbit (Weinreich & Wonderlin, 1987; Christian, Taylor & Weinreich, 1989*a*) and guinea-

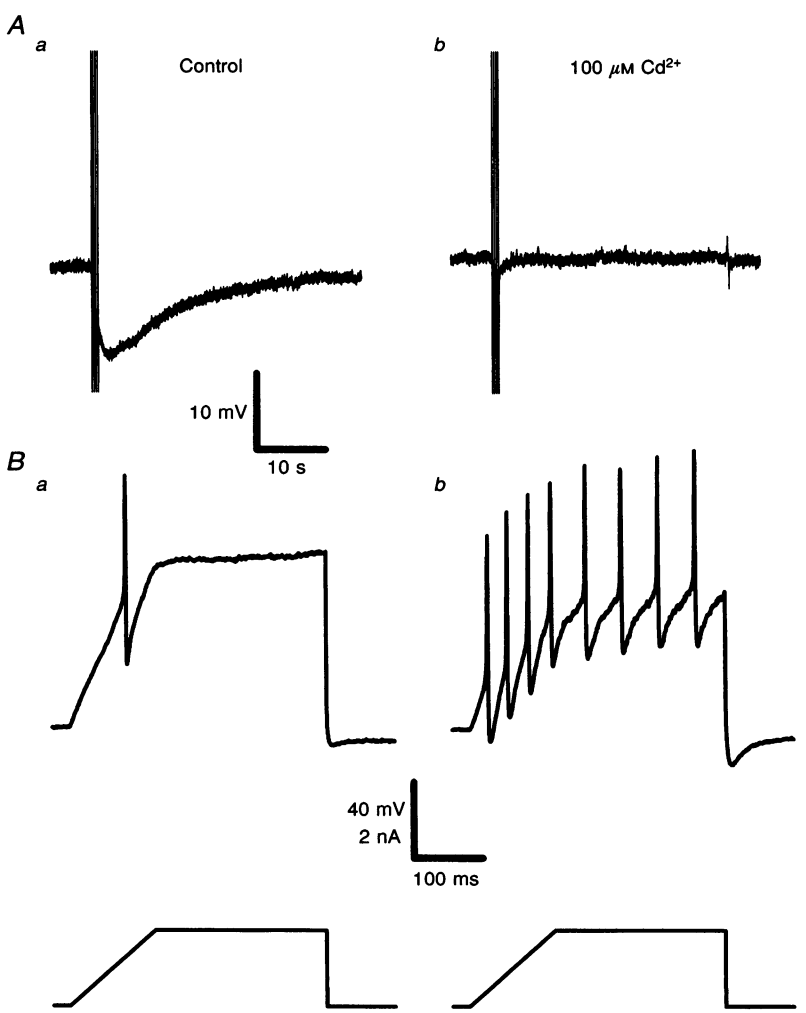

Figure 4. Block of the AHP_{slow} increases the excitability of a neurone
A, the AHP_{slow} elicited by four action potentials (produced by four depolarizing current pulses; 2 nA; 3 ms; 100 ms interspike interval), in the absence (*a*) and presence (*b*) of 100 μM Cd^{2+}. Cd^{2+} block of the AHP_{slow} (*Ab*) was reversible 2 min after superfusing the neurone with Cd^{2+}-free Locke solution. The action potentials and fast post-spike after-potentials are truncated. *Ba*, an applied current ramp (lower panel; 2 nA per 250 ms) followed by 500 ms of sustained current injection at the peak current attained during the ramp evokes a single action potential (upper trace). *Bb*, in the presence of Cd^{2+} (100 μM), the same stimulus results in repetitive firing of the neurone. All traces were recorded from the same neurone. The resting membrane potential was −70 mV.

pig (Undem & Weinreich, 1993) nodose neurones has been associated with an increase in neuronal excitability. Ferret nodose neurones also exhibit an increase in excitability when the AHP_{slow} is blocked. In these experiments changes in excitability were assessed by counting the number of action potentials elicited during a depolarizing current ramp (2 nA per 250 ms) followed by 500 ms of sustained current injection at the peak current attained during the ramp (Gold, Shuster & Levine, 1996) (Fig. 4*B*) under control conditions and while the AHP_{slow} was blocked using 100 μM cadmium (Fowler *et al.* 1985) (Fig. 4*A*). The number of action potentials elicited by this protocol in control (1 action potential in each of the 5 neurones tested) was significantly increased by 520% in the presence of 100 μM cadmium (5·2 ± 0·86 action potentials; $n = 5$; range, 3–8; Fig. 4*B*). The histamine effects in these neurones are a complex combination of membrane depolarization, increased input resistance and block of the AHP_{slow}. To isolate the effect of the AHP_{slow} on excitability, cadmium was used as a blocker of the AHP_{slow}. Cadmium (100 μM) had no effect on the resting membrane potential (< 2 mV) or membrane input resistance (< 2 MΩ) of these neurones ($n = 15$). The histamine-induced depolarization was unchanged in the presence of 100 μM cadmium (10 ± 1·0; $n = 10$; range, 6–16 mV) compared with control Locke solution (10 ± 0·9; $n = 10$; range, 6–15 mV). Nonetheless, a similar increase in

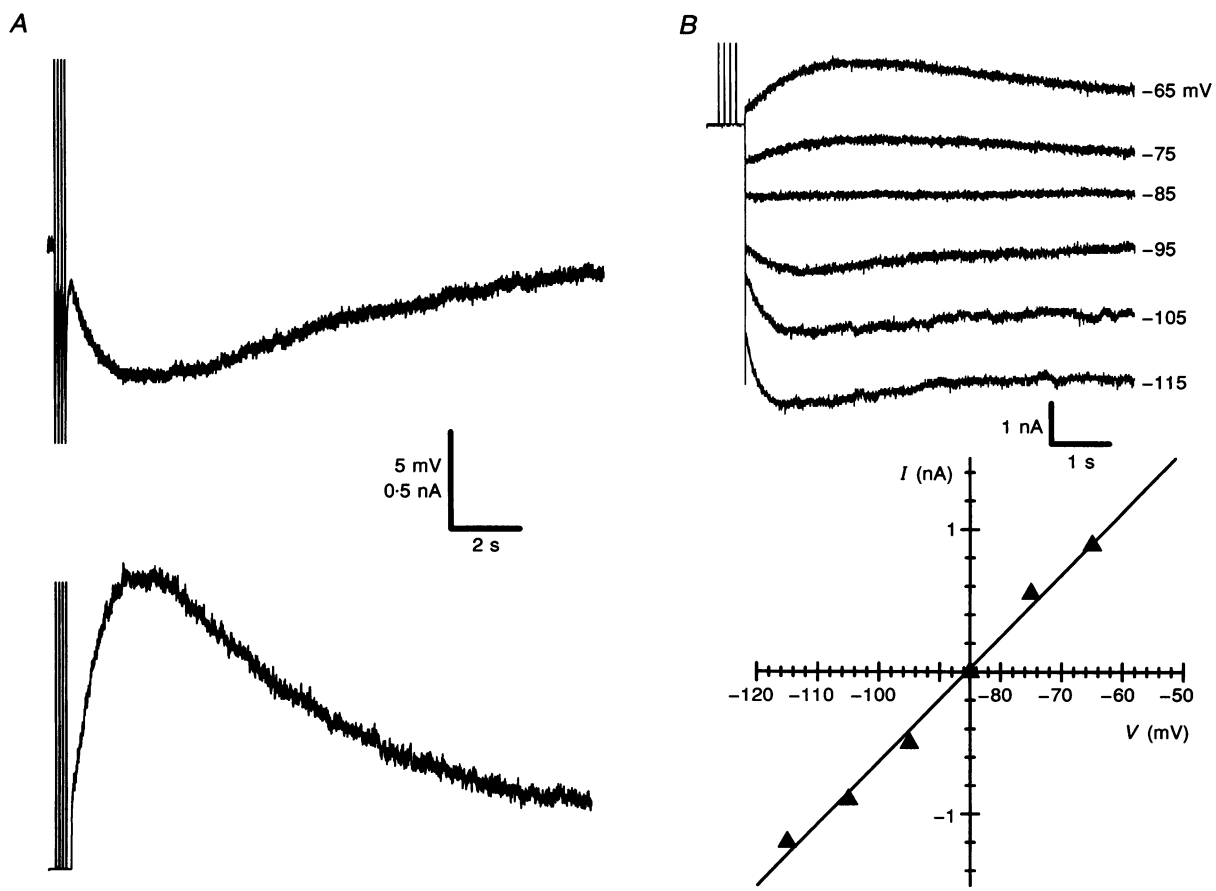

Figure 5. Recording of the AHP_{slow} and I_{AHP} from a single neurone

A (top trace), voltage trace from a current-clamp recording of an AHP_{slow} elicited by of four action potentials. Action potentials were produced by depolarizing current pulses (2 nA; 3 ms; 100 ms interspike interval). Resting potential was −65 mV. The action potentials and fast post-spike after-potentials are truncated. *A* (bottom trace), current trace of a hybrid voltage-clamp recording from the same neurone depicting the I_{AHP} elicited by four action potentials. The four upward deflections at the start of the trace reflect the 2 nA current pulses (truncated; 3 ms; 100 ms interspike interval) applied while in current-clamp mode to induce four action potentials. Following a latency of 100 ms after the last current pulse, the amplifier is switched to voltage-clamp mode. The resting potential during the current-clamp portion of this experiment was −65 mV; the holding potential during the voltage-clamp portion was −65 mV. *B* (top traces), superimposition of I_{AHP} traces from hybrid voltage-clamp recordings clamped to different holding potentials (−65, −75, −85, − 95, −105 and −115 mV). In all traces the 2 nA current stimulus pulses used to elicit the action potentials were applied in current-clamp mode with the neurone at the resting potential of −65 mV. *B* (bottom), plot of the *I–V* relationship for the I_{AHP} data from top traces. The data are fitted by a straight line ($r = 0·996$) with a V_{rev} value of −86 mV.

excitability was observed following histamine-induced block of the AHP_{slow}. The number of action potentials elicited by the ramp protocol in control (1 action potential in each of 5 neurones) was significantly increased by 640% in the presence of 10 μM histamine (6·4 ± 0·51 action potentials; $n = 5$; range, 5–8).

In rabbit and guinea-pig the AHP_{slow} results from activation of a potassium conductance, I_{AHP}. The current underlying the AHP_{slow} (I_{AHP}) was measured using the hybrid voltage-clamp technique (see Methods) (Fig. 5*A*, bottom panel). To determine the V_{rev} value for the I_{AHP}, a series of experiments with the neurone voltage clamped to different holding potentials were performed (Fig. 5*B*, top panel). The V_{rev} value for the I_{AHP} in ferret was −85 ± 1·68 mV ($n = 4$; range, −82 to −90 mV) implying that this is a potassium conductance (Fig. 5*B*).

Pharmacology of the histamine-induced depolarization and block of AHP_{slow}

The concentration–response relationship for the histamine-induced current was examined by voltage clamping the membrane potential to −60 mV and measuring the peak amplitude of the inward current (Fig. 6*B*). Histamine at concentrations ranging from 0·3 to 30 μM produced a concentration-dependent inward current. A semilogarithmic plot of peak current amplitude *versus* histamine concentration revealed a sigmoidal relationship that saturated at high concentrations; features indicative of a receptor-mediated interaction (Fig. 6*C*, ●). The currents were normalized to the amplitude of responses to saturating concentrations of histamine (⩾ 30 μM; I_{max}). The EC_{50} value estimated from a four-parameter logistic fit of the data ($n = 3$–10) was 2 μM (see Methods).

The concentration dependence of the histamine-mediated blockade of the AHP_{slow} (Fig. 6*A*) was assessed using three concentrations of histamine: 0·3, 3 and 30 μM, corresponding to low, intermediate and high concentrations necessary for inducing inward current. The concentration–response relationship for the block of AHP_{slow} is indistinguishable from that described for the histamine-induced inward current (Fig. 6*C*, △); its EC_{50} value was also estimated to be 2 μM.

Endogenous histamine activates three known histamine receptor subtypes, designated H_1, H_2 and H_3 (reviewed by Hill, 1990). All three of these receptor subtypes have been associated with neuronal depolarization. To determine which receptor subtype subserves these histamine-mediated effects, we applied agonists and antagonists selective for different histamine receptor subtypes. Antagonists were applied at concentrations 100 times greater than their dissociation constants (K_d).

Application of 10 μM 2-TH, an H_1-specific agonist, induced a membrane depolarization (5 ± 0·9 mV; $n = 6$; range, 3–8 mV; Fig. 7*B*). In contrast, bath application of either 10 μM impromidine or 10 μM R-α-MeHA, selective H_2 and H_3 receptor agonists, respectively, produced no measurable (< 1 mV) membrane potential changes ($n = 4$ for each agonist). We selected representatives of two distinct chemical classes of H_1 receptor antagonist to test further whether the receptor associated with the histamine-induced depolarization was of the H_1 subtype. Pyrilamine (100–500 nM) reversibly abolished the 10 μM histamine-induced depolarization by 100% in eleven of thirteen neurones (99 ± 0·8% blockade; $n = 13$; range, 92–100%; Fig. 7*A*). Similarly, 100 nM DPH completely prevented the depolarization induced by 10 μM histamine in ten of twelve neurones (98 ± 1·1% blockade; $n = 12$; range, 90–100%). The effect of 10 μM 2-TH was also reversibly blocked by 500 nM pyrilamine (100% block in 3 of 3 neurones; Fig. 7*B*). To identify this receptor definitively, we assessed the potency of pyrilamine antagonism on the histamine-induced inward current. Block by pyrilamine at 1, 3 and 10 nM was surmountable with increasing concentrations of histamine and subsequent Schild plot analysis revealed a pA_2 value of 9·7 (Fig. 7*C*), consistent with that for an H_1 receptor ($pA_2 = 9·1$; Hill, 1990) in other species. These results indicate that the histamine-induced inward current in ferret nodose neurones is mediated through the H_1 receptor subtype.

The pharmacological characterization for the histamine-induced block of the AHP_{slow} was pursued using a similar protocol. The AHP_{slow} was blocked by 10 μM 2-TH (48 ± 8·2% block; $n = 3$; range, 35–63% block) while affected little by 10 μM impromidine (3 ± 4·0%; $n = 3$; range, 0–11% block of AHP_{slow}) or 10 μM R-α-MeHA (13 ± 1·5%; $n = 3$; range, 11–16% block of AHP_{slow}), H_2 and H_3 receptor agonists, respectively (Fig. 8*C* and *D*). In the presence of 500 nM pyrilamine, 10 μM histamine produced only a 13 ± 9·8% block of the AHP_{slow} ($n = 3$; range, 0–32%); with 100 nM DPH, 10 μM histamine induced only a 2 ± 3·6% block ($n = 3$; range, 0–9%; see Fig. 8*E*). The effect of these antagonists were reversible (Fig. 8*F*). Thus, the block of the AHP_{slow}, like the membrane depolarization, appears to be mediated through activation of an H_1 receptor.

DISCUSSION

The major observation of this work is that histamine can increase the excitability of ferret vagal neurones by blocking two distinct potassium currents through activation of a single histamine receptor subtype. Activation of the histamine H_1 receptor subtype depolarizes the resting membrane potential and decreases the membrane conductance. Both these effects are brought about by a block of $I_{K(rest)}$. Histamine also blocks a potassium current underlying a post-spike slow after-hyperpolarization, the I_{AHP}. Block of the I_{AHP} profoundly enhances excitability by increasing the discharge characteristics of these neurones.

Are the effects of histamine on these two currents a result of modulation of a single type of K^+ channel? This is possible if I_{AHP} channels are open at rest and contribute to

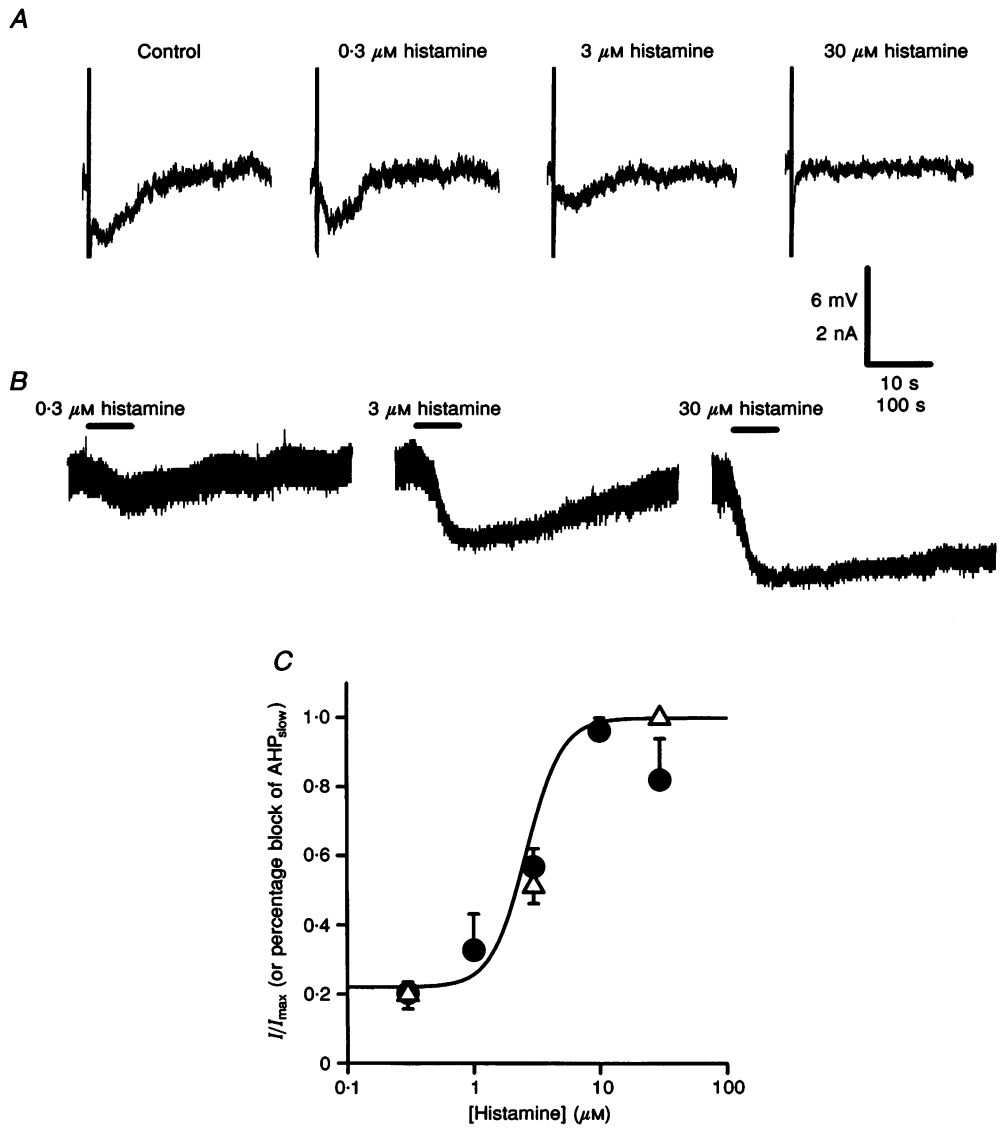

Figure 6. Relationship between histamine concentration and peak amplitude of the histamine-induced inward current or block of the AHP_{slow}

Concentration–response relationship between histamine (0, 0·3, 3 and 30 μM) and block of the AHP_{slow} recorded in the same neurone. *A*, the AHP_{slow}, elicited by four action potentials, was blocked by 0·3, 3 and 30 μM histamine in a concentration-dependent manner. The action potentials were produced by four depolarizing current pulses (3 nA; 3 ms; 100 ms interspike interval). Responses were recorded > 1 min after the start of histamine application with the neurone current clamped to resting membrane potential. The neurones were superfused with control Locke solution until the AHP_{slow} returned to control amplitude (> 10 min) between each histamine application. Resting membrane potential was −60 mV. The action potentials and fast post-spike after-potentials are truncated. *B*, representative current responses to 0·3, 3 and 30 μM histamine (60 s application bar) from a holding potential of −60 mV. The neurone was washed with control Locke solution for > 10 min before the next concentration of histamine was applied. *C*, semilogarithmic plot of the concentration–response relationship for the histamine-induced inward current (●; $n = 3$–10) or block of AHP_{slow} (△; $n = 3$ for each concentration). The currents were normalized to the amplitude of responses to saturating concentrations of histamine (⩾ 30 μM; I_{max}). Values are means ± S.E.M. The continuous line represents a logistic equation fitted to the data points for the inward current (see Methods; $EC_{50} = 2$ μM; slope factor = 3; $r = 0{\cdot}935$). The data points for the concentration–response relationship for the histamine-induced block of the AHP_{slow} are superimposed on the same graph (△). The AHP_{slow} values are not significantly different from the inward current values at the same concentration. Error bars where not visible are within symbols.

maintaining the resting membrane potential. Assessing whether these currents constitute separate entities is complicated because there are no known selective blockers for either of them. Apamin (1–100 nM) is a known blocker of the SK channel AHP_{slow} in some neurones (reviewed by Sah, 1996). In this concentration range, apamin does not block the AHP_{slow} in ferret, rabbit or guinea-pig nodose neurones (authors' unpublished observations). Insights as to whether these two channels are distinct may come from measurements of the single channel parameters for each of these currents. Ultimately molecular and structural data will be required to arrive at a definitive conclusion. At present,

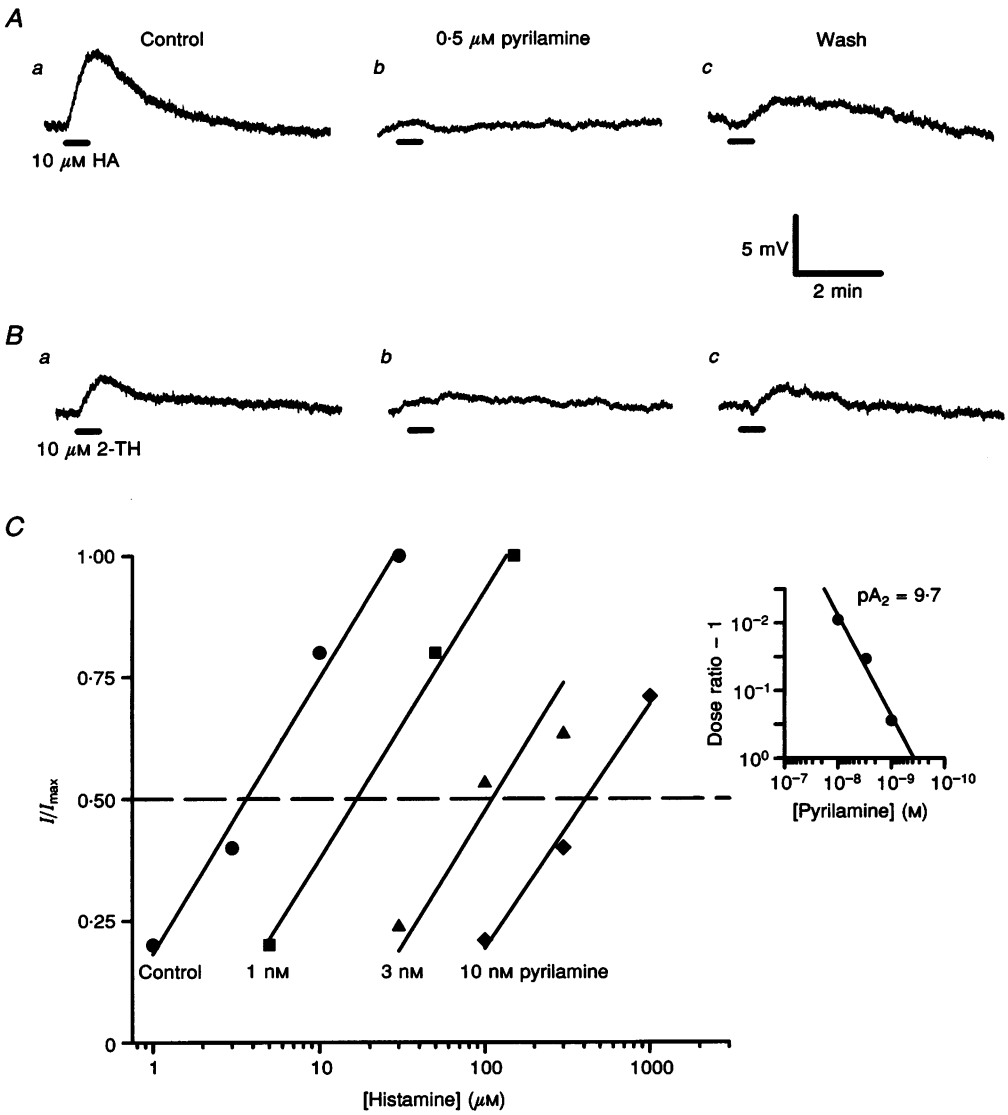

Figure 7. Block of histamine- or 2-TH-induced membrane depolarization by an H_1 receptor antagonist in a single ferret nodose neurone

A, histamine superfusion (10 μM; 30 s; horizontal bar) produces a membrane depolarization (*a*) that is blocked by 0·5 μM pyrilamine (Pyr), an H_1 receptor-specific antagonist (*b*). *Ac*, the histamine response partially recovers following a 30 min wash with drug-free Locke solution. *B*, in the same neurone application of the H_1 receptor-specific agonist 2-TH (10 μM; 30 s; horizontal bar) also produces a membrane depolarization (*a*). This effect is also blocked by Pyr (0·5 μM; *b*). *Bc*, partial recovery of the 2-TH response occurs following 30 min wash with drug-free Locke solution. In both experiments the neurone was superfused with Pyr for 2 min before application of histamine or 2-TH. The neurone was washed with normal Locke solution for at least 20 min between each histamine or 2-TH application. Resting membrane potential was −63 mV. *C*, concentration–response relationship for the histamine-induced depolarization in control Locke solution (●) or in Locke solution containing 1 nM (■), 3 nM (▲) or 10 nM (◆) Pyr recorded in a single neurone. Responses were normalized to maximal response measured in this neurone under control conditions (I_{max}). These data were fitted by a linear least-squares algorithm using the same estimated slope factor for all lines (Fieller's Theorem; Colquhoun, 1971). Schild plot analysis (inset) revealed a pA_2 value of 9·7 ($r = 0·9849$). The data were fitted by a linear least-squares algorithm.

we have indirect evidence implying that these potassium currents are, in fact, distinct. We have observed nodose neurones that are depolarized by histamine but do not possess a measurable AHP_{slow}, as well as nodose neurones, which exhibit an AHP_{slow} that is blocked by histamine, but are not depolarized by histamine. Furthermore, the AHP_{slow} is completely abolished in the presence of 100 μM cadmium (Fig. 4*A*), 1 mM cobalt or in nominally zero extracellular calcium (Fowler *et al.* 1985); however, none of these treatments affect the histamine-induced depolarization. Finally, chelation of intracellular calcium using BAPTA AM (20 μM) also abolishes the AHP_{slow} without affecting the histamine-induced depolarization (authors' unpublished observations). In the aggregate, these results are compatible with the interpretation that these two potassium currents are mediated by distinct potassium channels.

Histamine-induced depolarization

In > 80% of ferret nodose neurones, histamine application evokes a robust depolarization (10 ± 0·8 mV) driving the membrane potential towards spike threshold. In more than 75% of these histamine-sensitive neurones, this membrane depolarization was accompanied by a decrease in the membrane conductance. The V_{rev} for the histamine-induced depolarization was −84 ± 2·4 mV, a value near to the potassium V_{rev} in ferret nodose neurones (Jafri & Weinreich, 1996*b*). We further documented the importance of potassium as a charge carrier in this response by showing that the change in the histamine V_{rev} values produced by varying the extracellular potassium concentration over a sixfold range closely followed a Nernstian relationship (Fig. 3*E*). These results, along with the observation that a decrease in membrane conductance accompanies the histamine-induced depolarization, imply that histamine can cause membrane depolarization by blocking a population of potassium channels that are normally open at the resting membrane potential. The current flowing through these channels is designated $I_{K(rest)}$. Histamine-induced depolarizations mediated by a block of $I_{K(rest)}$ are not unique to vagal afferent neurones because this mechanism has been observed in various peripheral (Higashi *et al.* 1982; Nemeth, Ort & Wood, 1984; Christian, Undem & Weinreich, 1989*b*; Leal-Cardoso *et al.* 1993; Hutcheon, Puil & Spigelman, 1993; Christian *et al.* 1993) and central neurones (McCormick & Williamson, 1991; Reiner & Kamondi, 1994; Munakata & Akaike, 1994; Li & Hatton, 1996).

The size of a histamine-induced membrane depolarization when histamine receptors are coupled to $I_{K(rest)}$ should depend largely upon the magnitude of the neurone's resting conductance. This clearly seems to be the case with respect to nodose neurones in different species that have dissimilar resting membrane input conductances. In acutely isolated adult nodose neurones from ferret, rabbit and guinea-pig,

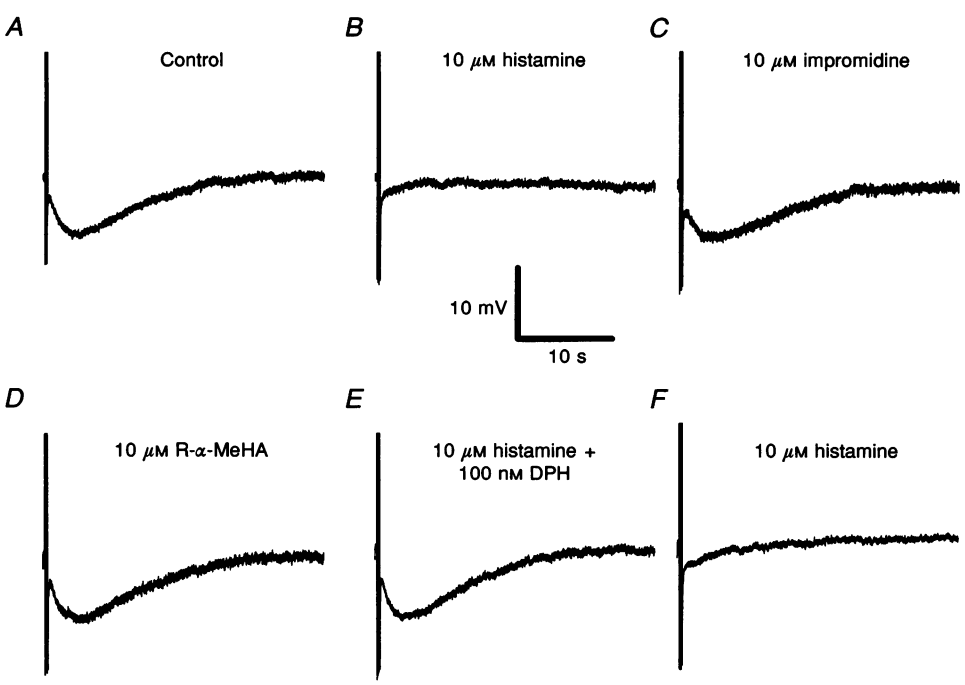

Figure 8. Histamine-induced block of the AHP_{slow} through activation of an H_1 receptor

An AHP_{slow} recorded from a single ferret nodose neurone under control conditions (*A*) or in the presence of different histamine receptor agonists and antagonists. Action potentials were evoked by four depolarizing current pulses (2 nA; 3 ms; 100 ms interspike interval). *B*, histamine (10 μM) blocked the AHP_{slow} while 10 μM impromidine (an H_2 receptor-specific agonist; *C*) or 10 μM R-α-MeHA (an H_3 receptor-specific agonist; *D*) had no effect. *E*, the H_1 receptor-specific antagonist DPH (100 nM) reversibly blocked the effect of histamine on the AHP_{slow}. *F*, after removal of DPH, histamine was again able to block the AHP_{slow}. The interval between traces was at least 5 min. Resting membrane potential was −56 mV.

the respective resting membrane input resistances and depolarizing responses to 10 μM histamine were: ~20 MΩ and 10 mV (current work), ~70 MΩ and 4 mV (Leal-Cardoso *et al.* 1993) and ~100 MΩ and 2 mV (Christian *et al.* 1993). This relatively direct reliance of the histamine response on the magnitude of the resting input conductance may not always occur because the efficacy of the presumed second messengers coupling receptor activation to K_{rest} channels may vary with cell type. The importance of histamine acting on $I_{K(rest)}$ may be particularly relevant under pathophysiological conditions where chemical-, mechanical- or allergen-induced inflammation can cause histamine release. Histamine, in turn, can sensitize sensory nerve endings to mechanical stimuli (Lee & Morton, 1993).

Histamine induced block of AHP_{slow}

Histamine reversibly abolished an AHP_{slow} that was present in > 80% of ferret nodose neurones. This action of histamine was concentration dependent (EC_{50} = 2 μM) and mediated by an H_1 receptor (see below). The properties of this AHP_{slow} are similar to those of the more extensively studied AHP_{slow} found in rabbit nodose neurones (Higashi, Morita & North, 1984; Fowler *et al.* 1985; Weinreich & Wonderlin, 1987; Leal-Cardoso *et al.* 1993). The V_{rev} values for the ferret I_{AHP} indicates that it is also likely to be produced by an outward flow of potassium ions. The AHP_{slow} contributes to spike frequency adaptation in these neurones (Fig. 4), and its modulation by histamine profoundly affects the pattern of action potential discharge. As in the case of histamine-induced depolarization, the effect of histamine on the AHP_{slow} is not novel to vagal afferents. Haas & Konnerth (1983) showed that an analogous slow after-potential exists in hippocampal CA3 neurones and that it was also blocked by histamine, although via the H_2 type of histamine receptor. In AH/type 2 myenteric neurones, histamine produces multiple effects similar to those observed in vagal afferents, namely, it depolarizes the resting membrane potential, increases the input resistance and blocks a post-spike after-hyperpolarization similar to the AHP_{slow} (Nemeth *et al.* 1984). Though H_1- and H_2-type histamine agonists and antagonists were used in this study, the pharmacological nature of the histamine receptors mediating these various membrane effects still remains unresolved.

Pharmacology of histamine effects

The pharmacological characterization of histamine's membrane effects recorded in ferret nodose neurones strongly indicates that they are mediated through activation of a single receptor subtype, namely the H_1 receptor. The concentration–response relationship for the histamine-induced depolarization was saturable at high concentrations and could be fitted by a sigmoid curve indicating that this effect is receptor mediated. The EC_{50} value of 2 μM is consistent with that expected for H_1 receptor activation (reviewed by Hill, 1990). The concentration–response

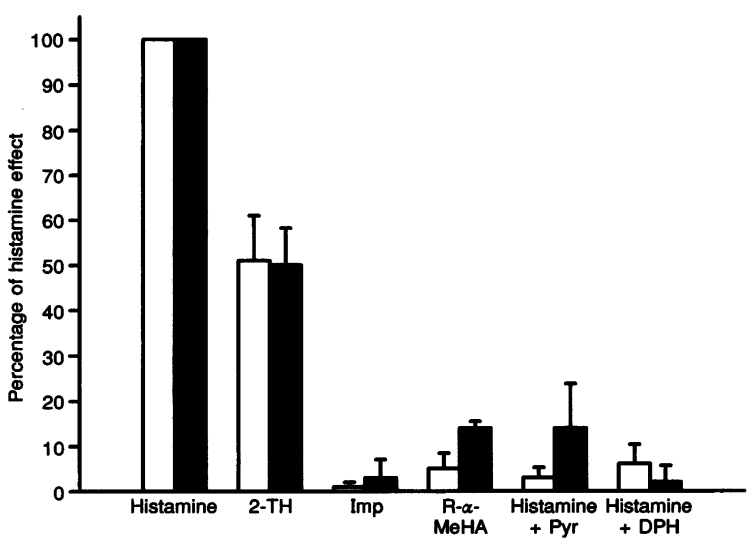

Figure 9. Histamine-induced inward currents or histamine block of the AHP_{slow} possess similar pharmacological profiles

The effects of selective histamine receptor agonists and antagonists were normalized to the effect of 10 μM histamine on either the inward current (□) or the block of the AHP_{slow} (■). The H_1 receptor-specific agonist 2-TH (10 μM; n = 6 for inward current and n = 3 for AHP_{slow} block) produces half the inward current that histamine does and is about half as effective as histamine at blocking the AHP_{slow}. The H_2 and H_3 receptor-specific agonists, impromidine (Imp; 10 μM; n = 4 and 3) and R-α-MeHA (10 μM; n = 4 and 3), respectively, were nearly equally ineffective in mimicking the effects of histamine. The H_1 receptor-specific antagonists, pyrilamine (Pyr; 0·5 μM; n = 13 and 3) or DPH (0·1 μM; n = 9 and 3) were equally effective at blocking both histamine effects. Error bars are S.E.M.

relationship for the histamine-mediated block of the AHP_{slow} also lies along the same curve indicating a similar concentration dependency. The effects of specific histamine receptor agonists and antagonists provide further evidence supporting the contention that both these histamine-mediated effects follow H_1 receptor activation. In ferret nodose neurones, 10 μM 2-TH, an H_1-specific agonist (reviewed by Hill, 1990), causes about a 5 mV depolarization, a value about one-half that produced by 10 μM histamine; 2-TH is also about half as effective as histamine in blocking the AHP_{slow} (Fig. 9). Pyrilamine and DPH represent two distinct chemical classes of H_1 receptor antagonists. Both these antagonists prevent histamine-induced membrane depolarization and block of the AHP_{slow}. In contrast, H_2 and H_3 receptor agonists, impromidine and R-α-MeHA, respectively, had no effect on either the histamine-induced membrane depolarization or the block of the AHP_{slow} (Fig. 9). Finally, the pA_2 value of 9·7 for the pyrilamine block of the histamine-induced depolarization is close to that reported for pyrilamine at many other native H_1 receptors (reviewed by Hill, 1990) and cloned H_1 receptors (Yamashita *et al.* 1991). In the aggregate, the pharmacological characterization of these two excitatory effects indicate that histamine acts through the H_1 receptor both to elicit a membrane depolarization and to block the AHP_{slow}.

How the H_1 receptor exerts control over $I_{K(rest)}$ and I_{AHP} remains unresolved. The divergence of the effector pathway may occur at any point beyond receptor activation. H_1 receptors may activate two or more second messengers to control the K^+ currents (Brown & Higashida, 1988). Alternatively, if the H_1 receptor were G protein linked it is possible the G_α subunit could control one current while the $G_{\beta\gamma}$ subunits would affect the other current. Future studies will be necessary to elucidate the underlying signalling components of this histamine system.

Physiological relevance of the effects of histamine

Histamine is an ubiquitous inflammatory autacoid commonly stored in mast cells associated with peripheral neurones (Olsson, 1966; Marshall & Waserman, 1995). Mast cells are located near peripheral sensory nerve endings (Stead, Tomioka, Quinonez, Simon, Felton & Bienenstock, 1987) and near their somata in sensory ganglia (Undem *et al.* 1993). Immunological activation of mast cells in the guinea-pig nodose ganglion can cause a membrane depolarization and decrease in spike frequency accommodation through block of the AHP_{slow} (Undem & Weinreich, 1993; Undem *et al.* 1993). If similar responses occur in peripheral nerve terminals following mast cell activation, they might contribute to the hyperactive behaviour of sensory nerve endings observed during inflammation (Riccio, Myers & Undem, 1996). Of particular pathophysiological interest is the possible involvement of these histamine-mediated increases in excitability in vagal afferent nerve endings to the airways where local axon reflexes may contribute to many symptoms of airway diseases, such as asthma (Ellis & Undem, 1992).

Modulation of multiple conductances by activation of a single autacoid receptor subtype appears to be a common motif used by ferret nodose neurones. Substance P activates an outward potassium current and also inhibits a hyperpolarization-activated depolarizing current (I_h). It is interesting to note that the modulation of these two substance P-activated currents is mediated through one tachykinin receptor, the NK1 subtype (Jafri & Weinreich, 1996*a*).

In conclusion, we have demonstrated that activation of the H_1 receptor subtype is responsible for a membrane depolarization resulting from block of a resting potassium conductance. In addition H_1 receptor activation blocks a post-spike slow after-hyperpolarization that contributes to spike frequency accommodation. In this manner these two histamine-mediated mechanisms can produce potentially synergistic effects on the excitability and frequency encoding of impulses in these afferent neurones.

Baccaglini, P. I. & Hogan, P. G. (1983). Some rat sensory neurons in culture express characteristics of differentiated pain sensory cells. *Proceedings of the National Academy of Sciences of the USA* **80**, 594–598.

Brown, D. A. & Higashida, H. (1988). Inositol 1,4,5-trisphosphate and diacylglycerol mimic bradykinin effects on mouse neuroblastoma × rat glioma hybrid cells. *Journal of Physiology* **397**, 185–207.

Christian, E. P., Taylor, G. E. & Weinreich, D. (1989*a*). Serotonin increases excitability of rabbit C-fiber neurons by two distinct mechanisms. *Journal of Applied Physiology* **67**, 584–591.

Christian, E. P., Undem, B. J. & Weinreich, D. (1989*b*). Endogenous histamine excites neurones in the guinea-pig superior cervical ganglion *in vitro*. *Journal of Physiology* **409**, 297–312.

Christian, E. P., Togo, J. A., Naper, K. E., Koschorke, G., Taylor, G. E. & Weinreich, D. (1993). A retrograde labeling technique for the functional study of airway-specific visceral afferent neurons. *Journal of Neuroscience Methods* **47**, 147–160.

Coleridge, J. C. G. & Coleridge, H. M. (1977). Afferent C-fibers and cardiorespiratory chemoreflexes. *American Review of Respiratory Disease* **115**, 251–260.

Colquhoun, D. (1971). *Lectures on Biostatistics*, pp. 287–297. Oxford University Press, New York.

Ellis, J. L. & Undem, B. J. (1992). Antigen-induced enhancement of noncholinergic contractile responses to vagus nerve and electrical field stimulation in guinea pig isolated trachea. *Journal of Pharmacology and Experimental Therapeutics* **262**, 646–653.

Fowler, J. C., Greene, R. & Weinreich, D. (1985). Two calcium-sensitive spike after-hyperpolarizations in visceral sensory neurones of the rabbit. *Journal of Physiology* **365**, 59–75.

Gold, M. S., Shuster, M. J. & Levine, J. D. (1996). Role of a slow Ca^{2+}-dependent afterhyperpolarization in prostaglandin E_2-induced sensitization of cultured rat sensory neurons. *Neuroscience Letters* **205**, 161–164.

Haas, H. L. & Konnerth, A. (1983). Histamine and noradrenaline decrease calcium-activated potassium conductance in hippocampal pyramidal cells. *Nature* **302**, 432–434.

HIGASHI, H., MORITA, K. & NORTH, R. A. (1984). Calcium-dependent after-potentials in visceral afferent neurones of the rabbit. *Journal of Physiology* **355**, 479–492.

HIGASHI, H., UEDA, N., NISHI, S., GALLAGHER, J. P. & SHINNICK-GALLAGHER, P. (1982). Chemoreceptors for serotonin (5-HT), acetylcholine (ACh), bradykinin (BK), histamine (H) and gamma-aminobutyric acid (GABA) on rabbit visceral afferent neurons. *Brain Research Bulletin* **8**, 23–32.

HILL, S. J. (1990). Distribution, properties, and functional characteristics of three classes of histamine receptor. *Pharmacological Reviews* **42**, 45–83.

HUTCHEON, B., PUIL, E. & SPIGELMAN, I. (1993). Histamine actions and comparison with substance P effects in trigeminal neurons. *Neuroscience* **55**, 521–529.

JAFRI, M. S. & WEINREICH, D. (1996*a*). Substance P regulation of I_K and I_h decreases excitability of ferret vagal sensory neurons via a NK-1 receptor. *Journal of Neuroscience* **22**, 1800 (abstract).

JAFRI, M. S. & WEINREICH, D. (1996*b*). Substance P hyperpolarizes vagal sensory neurones of the ferret. *Journal of Physiology* **493**, 157–166.

LEAL-CARDOSO, H., KOSCHORKE, G. M., TAYLOR, G. & WEINREICH, D. (1993). Electrophysiological properties and chemosensitivity of acutely isolated nodose ganglion neurons of the rabbit. *Journal of the Autonomic Nervous System* **45**, 29–39.

LEE, L.-Y. & MORTON, R. F. (1993). Histamine enhances pulmonary C-fiber responses to capsaicin and lung inflation. *Respiration Physiology* **93**, 83–96.

LI, Z. & HATTON, G. I. (1996). Histamine-induced prolonged depolarization in rat supraoptic neurons: G-protein-mediated, Ca^{2+}-independent suppression of K^+ leakage conductance. *Neuroscience* **70**, 145–158.

MARSHALL, J. S. & WASERMAN, S. (1995). Mast cells and the nerves – potential interactions in the context of chronic disease. *Clinical and Experimental Allergy* **25**, 102–110.

MCCORMICK, D. A. & WILLIAMSON, A. (1991). Modulation of neuronal firing mode in cat and guinea pig LGNd by histamine: Possible cellular mechanisms of histaminergic control of arousal. *Journal of Neuroscience* **11**, 3188–3199.

MUNAKATA, M. & AKAIKE, N. (1994). Regulation of K^+ conductance by histamine H_1 and H_2 receptors in neurones dissociated from rat neostriatum. *Journal of Physiology* **480**, 233–245.

NEMETH, P. R., ORT, C. A. & WOOD, J. D. (1984). Intracellular study of effects of histamine on electrical behaviour of myenteric neurones in guinea-pig small intestine. *Journal of Physiology* **355**, 411–425.

OLSSON, Y. (1966). Mast cells in the nervous system. *International Review of Cytology* **24**, 27–70.

REINER, P. B. & KAMONDI, A. (1994). Mechanisms of antihistamine-induced sedation in the human brain: H_1 receptor activation reduces a background leakage potassium current. *Neuroscience* **59**, 579–588.

RICCIO, M. M., MYERS, A. C. & UNDEM, B. J. (1996). Immunomodulation of afferent neurons in guinea-pig isolated airway. *Journal of Physiology* **491**, 499–509.

SAH, P. (1996). Ca^{2+}-activated K^+ currents in neurones: types, physiological roles and modulation. *Trends in Neurosciences* **19**, 150–154.

STEAD, R. H., TOMIOKA, M., QUINONEZ, G., SIMON, G. T., FELTON, S. Y. & BIENENSTOCK, J. (1987). Intestinal mucosal mast cells in normal and nematode-infected rat intestines are in intimate contact with peptidergic nerves. *Proceedings of the National Academy of Sciences of the USA* **84**, 2975–2979.

UNDEM, B. J., HUBBARD, W. & WEINREICH, D. (1993). Immunologically induced neuromodulation of guinea pig nodose ganglion neurons. *Journal of the Autonomic Nervous System* **44**, 35–44.

UNDEM, B. J. & RICCIO, M. M. (1997). Activation of airway afferent nerves. In *Asthma*, ed. BARNES, P. J., GRUNSTEIN, M. M., LEFF, A. & WOOLCOCK, A. J. Lippincott-Raven Publishers, Philadelphia (in the Press).

UNDEM, B. J. & WEINREICH, D. (1993). Electrophysiological properties and chemosensitivity of guinea pig nodose ganglion neurons *in vitro*. *Journal of the Autonomic Nervous System* **44**, 17–34.

WASSERMAN, S. I. (1994). Mast cells and airway inflammation in asthma. *American Journal of Respiratory and Critical Care Medicine* **150**, S39–41.

WEINREICH, D. (1986). Bradykinin inhibits a slow spike afterhyperpolarization in visceral sensory neurons. *European Journal of Pharmacology* **132**, 61–63.

WEINREICH, D. & WONDERLIN, W. F. (1987). Inhibition of calcium-dependent spike after-hyperpolarization increases excitability of rabbit visceral sensory neurones. *Journal of Physiology* **394**, 415–427.

YAMASHITA, M., FUKUI, H., SUGAMA, K., HORIO, Y., ITO, S., MIZUGUCHI, H. & WADA, H. (1991). Expression cloning of a cDNA encoding the bovine histamine H_1 receptor. *Proceedings of the National Academy of Sciences of the USA* **88**, 11515–11519.

Acknowledgements

The authors wish to thank Drs Brad Undem and Edward Christian for their constructive suggestions on an earlier draft of this manuscript. This work was supported by NIH grant NS22069.

Author's email address

D. Weinreich: dweinrei@umabnet.ab.umd.edu

Received 11 March 1997; accepted 13 June 1997.